SHIP IMPACT MODELING OF UNDERWATER EXPLOSION

Andrzej Grządziela

Polish Naval Academy, Mechanical Electrical Faculty
Śmidowicza Street 69, 81-103 Gdynia, Poland
tel.: +48 58 6262635, fax: +48 58 6262648
e-mail: a.grzadziela@wp.pl

Abstract

Ship shock tests have been conducted for shock qualification of hull integrity and proper operation systems and subsystems. The ship shock trial identifies design and construction and it also validates shock hardening criteria. The main problem is that ship shock trials are costly. Numerical modeling and simulation, using FEM, may provide information to look into the details of fluid model, dynamic characteristics of ship hull and its internal component. The ship shock modeling and simulation has been performed and the predicted results were compared with ship shock test data made into sea trials. The preliminary studies of shock analysis approach are presented and the important parameters are discussed.

The course of pressure changes in the shock wave and the acceleration of the ship hull during an underwater explosion in a fixed point, coating elements with chosen junction forces (example), designation of degrees of freedom of rectangular plate, simplified diagram of interactions in the process of detention in the hull of a ship, analysis of the acceleration of the Newmark method, calculations based on central difference method, schematic anchor launch, layout of the apparatus and the conditions for an explosion, the course of the accelerations recorded in the ship's hull, The course of simulation of the acceleration are presented in the paper.

Keywords: ship hull, simulation, underwater explosion

1. Introduction

The Underwater explosion is a process that takes place sequentially as well as in parallel with natural phenomena, leading to a system imbalance, which consists of an explosive material and the surrounding liquid medium. This process is accompanied by chemical and physical reactions, release of large quantities of heat, gas formation and energy transmission in a relatively short time.

The first step of the underwater detonation process is the combustion of the explosive material, resulting in a detonation wave representing the surface of discontinuity and the formation of gas in the process of combustion. Established detonation wave propagates from the centre of the detonation to the surface of gas bubble and transmit energy to the adjacent water molecules. The gas takes the form of a bubble and moves upwards with a particular speed. The bubble may not exceed gas pressure of 14 000 MPa and a temperature of 3300 K [1]. Such large pressures give rise to the effect of water compressibility and thus the compression zone, which generates a pressure wave, which is often referred to as a shock wave. Front of this wave moves in the initial period of approximately 2.5 microseconds with the detonation velocity (about 6000 - 8000 m/s), and after a few milliseconds to a top speed (speed of sound) in water (about 1500 m/s) [1]. During this time the wave front moves a distance of several dozen meters.

Activity of the pressure wave and the expansion of gases in the bubble cause increase in the size and movement of water molecules at a speed of up to 600 - 800 m/s [1]. Since the velocity of expansion of the bubble is less than the speed of the pressure wave, separation of the front wave from the surface of the bubble follows. With the increase in the size of the bubble, the pressure inside it decreases. At the time of levelling in the amounts of the pressure inside the bubble and of the hydrostatic pressure, it will continue to increase its size. This inertia is caused by water molecules, which was attributed to kinetic energy. The diameter of the bubble grows until the internal pressure will be approximately 20% of the hydrostatic pressure.

The next step is the process of return of water molecules in the gas towards the centre of the sphere. As a result, the ball reduces its volume to the minimum value. This moment means the completion of the so called first pulse.

The pulse process occurs repeatedly until the gas bubble will flow to the surface. Hence, the number of pulses depends, inter alia, on the draft of the explosive charge. The way that nature of pressure changes in a fixed point of the water is shown in Fig. 1.

Pulsation period of each successive sphere gas is different. According to [3] it depends on the depth of the epicentre of the outbreak and the mass of the explosive material. In the draft of explosives:

$$H < 1.2\sqrt[3]{W}, \tag{1}$$

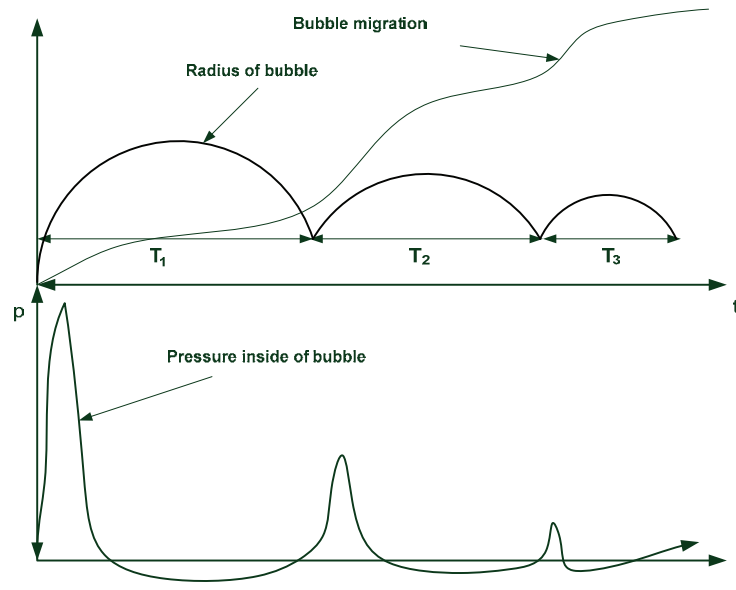where W is weight of the load of TNT [kg].

Fig. 1. The course of pressure changes in the shock wave and the acceleration of the ship hull during an underwater explosion in a fixed point [2]

Gas bubble will appear on the surface of the reservoir after the first pulse. According to [4], the period of first pulse is as follows:

$$T_1 = 0.3 \frac{\sqrt[3]{W}}{1+0.1H}. \tag{2}$$

Typically, the period of the second pulsation of gas bubble, T2, is in the range of 70-80% of the first one, T1, while the third pulsation period is about 50% of T1. The maximum radius of the gas bubble occurs during the first pulsation. It is calculated by the following empirical relationship [4]:

$$R_{max} = 1.53 \sqrt[3]{\frac{W}{1+0.1H}} [m]. \tag{3}$$

During the expansion of the gas bubble, which occurs as a result of the impact of the pressure wave from it adjacent, kinetic energy is transferred to water molecules. They begin to move with a certain speed, after which the transfer of energy to the next layers of water follows, causing the loss in speed [3]. It is assumed that the speed of water molecules is a function of maximum pressure on the front of the shock wave (p_{max}):

$$V_w = 0.7 \; p_{max} . \tag{4}$$

In the case of TNT, the maximum pressure resulting from TNT detonation presents the following relationship, (Cole [1]):

$$p_{max} = 523 \left(\frac{\sqrt[3]{W}}{R} \right)^{1.13} 10^5 \quad [Pa] , \tag{5}$$

where:
W - weight of the TNT [kg],
R - distance [m].

Besides the value of the maximum pressure, function describing the change in pressure over time is also important. Its course is approximated by an exponential function of the form:

$$p(t) = \left(K_1 \cdot \left(\frac{\sqrt[3]{W}}{R} \right)^{A_1} \right) e^{-(t-t_o)/\theta} \quad [MPa] , \tag{6}$$

where:
t_o - the time from the moment of first contact with the object of the pressure wave [ms],
$\theta = K_2 \cdot W^{1/3} \cdot \left(W^{1/3} / R \right)^{A_2}$ - Time constant [ms].

Time constant, including the factors given by Cole, is calculated as follows:

$$\theta = \sqrt[3]{W} \left[\frac{\sqrt[3]{W}}{R} \right]^{(-0.22)} 9.3 \cdot 10^{-5} \; [s] . \tag{7}$$

The maximum value of pressure prevailing at the front of the shock wave is not the only parameter that determines the effectiveness of its action. Consideration should also be taken about the stock of its impact. Both parameters are directly related through a relationship called the pulse pressure shock wave. Its value is calculated as follows [4]:

$$I(t,r) = \int_0^t p(t,r) dt \quad [Pa \; s] . \tag{8}$$

Often, calculated from a simplified relationship of the form:

$$I = p_{max} \cdot \theta \tag{9}$$

or according to the formula by Cole (for TNT):

$$I = 5768 \frac{(W)^{0.63}}{r^{0.89}} [Pa \cdot s] . \tag{10}$$

This formula allows calculating the pressure pulse shock wave during the first pulse on the assumption that the explosion took place away from the seabed and sea surface. Impulses from the subsequent pressure pulses are much weaker. In case of a second pulse value is approximately five times less than the pulse of the first one.

2. The impact of the detonation on the hull of the ship

As a result of underwater explosion, the pressure wave reaches the hull of the ship. Wave's profile is described by a well-known function. Integrating the pressure existing behind the front of the shock wave on the submerged hull elements, yields forces which, according to the theory of MES are reduced to the element's nodes - Fig. 2.
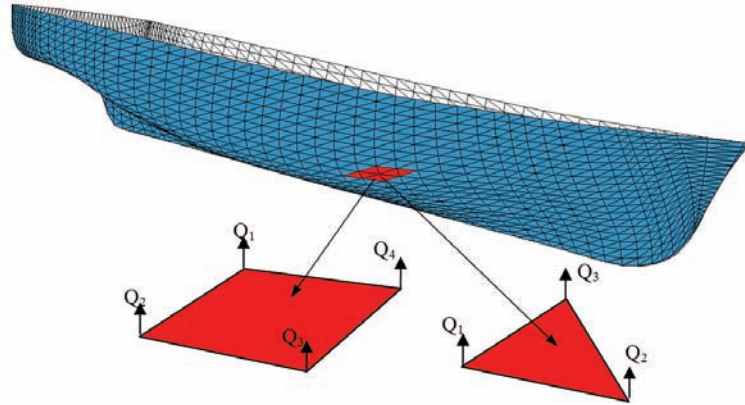
Fig. 2. Coating elements with chosen junction forces (example)

For further calculations the following assumptions will hold [5]:

- hull coating is digitized by plated, isoparametric elements, forming a grid describing the geometry of the hull,
- discrete components have a constant thickness,
- displacement point of the plate is a set constant, i.e. the deflection.

In case of the rectangular plate element for which the designation in the local coordinate system is shown on Fig. 3, each of the four nodes has three degrees of freedom, i.e. displacement and two rotations. The first index indicates the node number, the second – number of the degree of freedom in the node (1 - translational displacement, 2, 3 - rotational displacement).

According to the FEM theory, displacement of any point on the plate is approximated by the so-called. shape function. Due to the fact that the given element has 12 degrees of freedom, shape function will be a polynomial of arity 12. The deflection inside the element will be described as follows:

$$q_1(x_e, y_e) = \left[1, x_e, y_e, x_e^2, x_e y_e, y_e^2, x_e^3, x_e^2 y_e, x_e y_e^2, y_e^3, x_e^3 y_e, x_e y_e^3\right] \cdot \mathbf{a}, \tag{11}$$

or:

$$q_1(x_e, y_e) = \mathbf{\Phi} \cdot \mathbf{q}, \tag{12}$$

where:

$\mathbf{a}$ - vector of coefficients to be determined,
$\mathbf{\Phi}$ - matrix of the shape function,
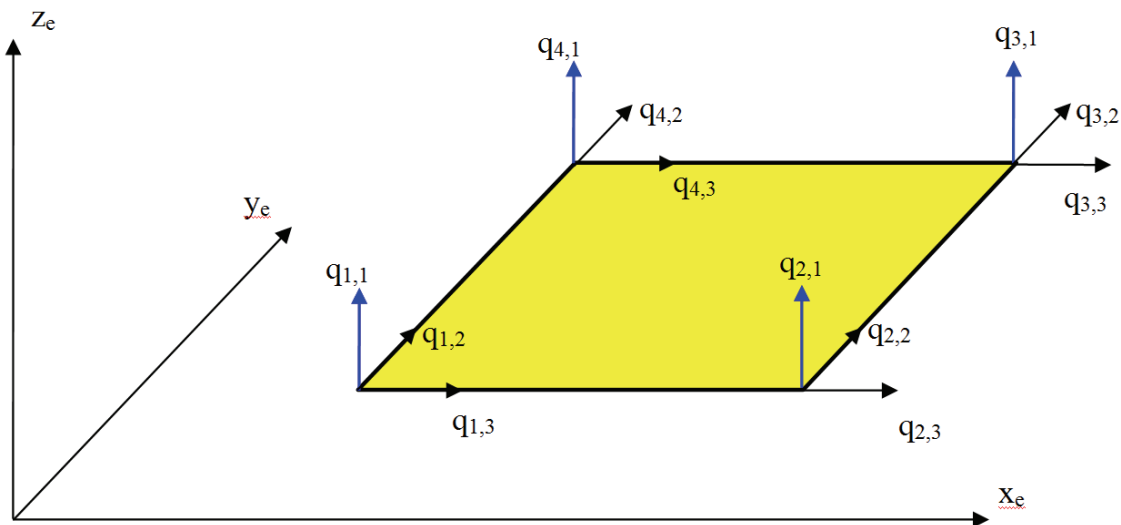$\mathbf{q}$ - vector of generalized nodal displacements.

Fig. 3. Designation of degrees of freedom of rectangular plate

Simplifying, the matrix takes the form:

$$\Phi = \left[1, x_e, y_e, x_e^2, x_e y_e, y_e^2, x_e^3, x_e^2 y_e, x_e y_e^2, y_e^3, x_e^3 y_e, x_e y_e^3\right] \cdot H^{-1},$$ (13)

where H is as follows:

$$H = \begin{bmatrix}
1 & x_{e1} & y_{e1} & x_{e1}^2 & x_{e1}y_{e1} & y_{e1}^2 & x_{e1}^3 & x_{e1}^2 y_{e1} & x_{e1}y_{e1}^2 & y_{e1}^3 & x_{e1}^3 y_{e1} & x_{e1}y_{e1}^3 \\
0 & 0 & 1 & 0 & x_{e1} & 2y_{e1} & 0 & x_{e1}^2 & 2x_{e1}y_{e1} & 3y_{e1}^2 & x_{e1}^3 & 3x_{e1}y_{e1}^2 \\
0 & -1 & 0 & -2x_{e1} & y_{e1} & 0 & -3x_{e1}^2 & -2x_{e1}y_{e1} & -x_{e1}^2 & 0 & -3x_{e1}^2 y_{e1} & -y_{e1}^2 \\
1 & x_{e2} & y_{e2} & x_{e2}^2 & x_{e2}y_{e2} & y_{e2}^2 & x_{e2}^3 & x_{e2}^2 y_{e2} & x_{e2}y_{e2}^2 & y_{e2}^3 & x_{e2}^3 y_{e2} & x_{e2}y_{e2}^3 \\
0 & 0 & 1 & 0 & x_{e2} & 2y_{e2} & 0 & x_{e2}^2 & 2x_{e2}y_{e2} & 3y_{e2}^2 & x_{e2}^3 & 3x_{e2}y_{e2}^2 \\
0 & -1 & 0 & -2x_{e2} & y_{e2} & 0 & -3x_{e2}^2 & -2x_{e2}y_{e2} & -x_{e2}^2 & 0 & -3x_{e2}^2 y_{e2} & -y_{e2}^2 \\
1 & x_{e3} & y_{e3} & x_{e3}^2 & x_{e3}y_{e3} & y_{e3}^2 & x_{e3}^3 & x_{e3}^2 y_{e3} & x_{e3}y_{e3}^2 & y_{e3}^3 & x_{e3}^3 y_{e3} & x_{e3}y_{e3}^3 \\
0 & 0 & 1 & 0 & x_{e1} & 2y_{e1} & 0 & x_{e1}^2 & 2x_{e1}y_{e1} & 3y_{e1}^2 & x_{e1}^3 & 3x_{e1}y_{e1}^2 \\
0 & -1 & 0 & -2x_{e1} & y_{e1} & 0 & -3x_{e1}^2 & -2x_{e1}y_{e1} & -x_{e1}^2 & 0 & -3x_{e1}^2 y_{e1} & -y_{e1}^2
\end{bmatrix}.$$

The values of the forces reduced to the nodes of the element (i = 1-4) can be determined using the following formula:

$$Q_i^e = \int_{\Omega_e} \varphi_i p(x_e, y_e)\, d\Omega ,$$ (14)

where:

φ_I - shape functions,

$p(x_e, y_e)$ - continuous load on the local element,

Ω_e - element field.

If we present the load as a continuous linear combination of shape functions and nodal values, we get:

$$Q_i^e = \int_{\Omega_e} \varphi_i \begin{bmatrix} \varphi_1 & \varphi_2 & \varphi_3 & \varphi_4 \end{bmatrix} d\Omega \begin{bmatrix} p_1 \\ p_2 \\ p_3 \\ p_4 \end{bmatrix}.$$ (15)

Integration is performed numerically in a standardized coordinate system. Apply the following procedure (it takes to account any shape and size of the item):

$$\int_{\Omega e} \varphi_i d\Omega = \int_{-1}^{1}\int_{-1}^{1} \varphi_i(s,t)\det J\, ds\, dt ,$$ (16)

where:

J - Jacobian transformation,

t, s - the coordinates of a standard coordinate system.

In the case of continuous load with a high gradient, one should take a greater number of points inside the element and use a denser mesh in order to obtain the appropriate accuracy of calculations. After calculating the nodal forces in local coordinates of each element, one must transpose those into a common global system with the formula:

$$\tilde{Q}_i^e = C \cdot Q_i^e ,$$ (17)

where C is the cosine matrix. In case, where described the elements have the three degrees of freedom in the node, the transposition is done using the following cosine matrix:

$$C = \begin{bmatrix} c' & 0 & 0 & 0 \\ 0 & c' & 0 & 0 \\ 0 & 0 & c' & 0 \\ 0 & 0 & 0 & c' \end{bmatrix},$$ (18)

where:

$$c' = \begin{bmatrix} \cos\alpha_{31} & \cos\alpha_{32} & \cos\alpha_{33} & 0 & 0 & 0 \\ 0 & 0 & 0 & \cos\alpha_{11} & \cos\alpha_{12} & \cos\alpha_{13} \\ 0 & 0 & 0 & \cos\alpha_{21} & \cos\alpha_{22} & \cos\alpha_{23} \end{bmatrix}.$$

Angles $\alpha_{i,j}$ (i=1-3, j=1-3), specify the location of the axes of the local elements. Entries in the cosine matrix are determined during integration, where the Jacobian transformation is calculated.

3. Model of the dynamic interaction of underwater detonation

Analyzing the dynamic effects of underwater explosion should be considered as a second Lagrange equation, in which the effects of detonation are the RHS [6]. Fig. 4 shows schematically the types of interactions occurring.
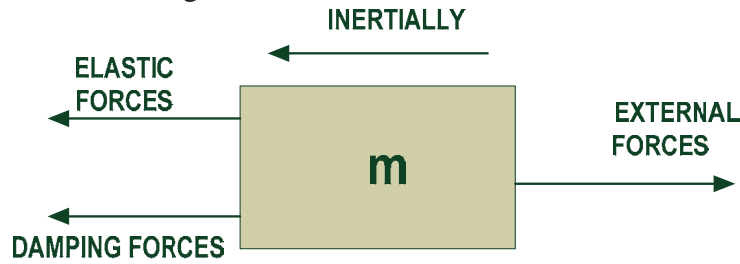

Fig. 4. Simplified diagram of interactions in the process of detention in the hull of a ship

Power equality expressing the second Lagrange equation can be presented as:

$$f_I + f_D + f_S = p(t), \tag{19}$$

where:
$f_I = M\ddot{u}(t)$,
$f_D = C\dot{u}(t)$,
$f_S = Ku(t)$.

This yields:

$$M\ddot{u}(t) + C\dot{u}(t) + Ku(t) = p(t), \tag{20}$$

where:
M - matrix of inertia,
C - matrix of damping coefficients,
K - stiffness matrix,
$u(t)$ - change in time (displacement),
$\dot{u}(t)$ - speed at the particular time (velocity),
$\ddot{u}(t)$ - acceleration,
$p(t)$ - vector of external forces.

The equation of motion depends on the time for which the discretization is needed. The equation of motion can be solved in two ways: implicit and explicit method. In the implicit method (e.g., the Newmark method) the equation of motion is solved in time . (e.g. at the end of the current time step), then the equation of motion becomes:

$$M_{n+1}\ddot{u}(t)_{n+1} + C_{n+1}\dot{u}(t)_{n+1} + K_{n+1}u(t)_{n+1} = p(t)_{n+1}. \tag{21}$$

In the explicit method (e.g. central difference method) the equation of motion is solved in time. (e.g. at the beginning of current time step), then the equation of motion becomes:

$$M_n\ddot{u}(t)_n + C_n\dot{u}(t)_n + K_nu(t)_n = p(t)_n. \tag{22}$$

The Newmark method assumes a linear change in acceleration – Fig. 5.

Then the speed:

$$\dot{u}_{n+1} = \dot{u}_n + \frac{\Delta t}{2}\ddot{u}_n + \frac{\Delta t}{2}\ddot{u}_{n+1}, \tag{23}$$

$$u_{n+1} = u_n + \dot{u}_n\Delta t + \frac{\Delta t^2}{3}\ddot{u}_n + \frac{\Delta t^2}{6}\ddot{u}_{n+1}. \tag{24}$$

displacement:

Displacement at t_{n+1}:

$$(\frac{6}{\Delta t^2}M_{n+1} + \frac{3}{\Delta t}C_{n+1} + K_{n+1})u_{n+1} = p_{n+1} + M_n(\frac{6}{\Delta t^2}u_n + \frac{6}{\Delta t}\dot{u}_n + 2\ddot{u}_n) + C_n(\frac{3}{\Delta t}u_n + 2\dot{u}_n + \frac{\Delta t}{2}\ddot{u}_n). \tag{25}$$
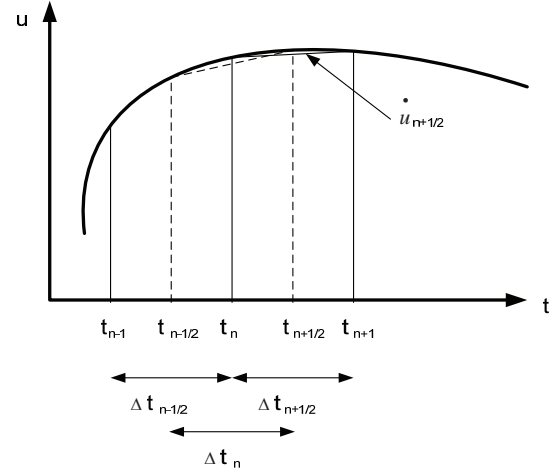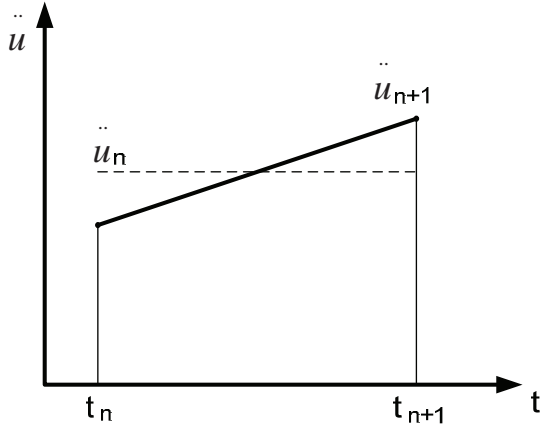
Fig. 5. Analysis of the acceleration of the Newmark method Fig. 6. Calculations based on central difference method

Stiffness matrix is on LHS as in cases of forced nonlinear iterations and the matrix inversion. It is a costly process and therefore, is a drawback of the method. Its advantage is the stability of the solution. The central difference method assumes a linear variation of displacement - Fig. 6. Then we define velocity as:

$$\dot{u}_{n+1/2} = \frac{1}{\Delta t_{n+1/2}}(u_{n+1} - u_n), \tag{26}$$

and acceleration as:

$$\ddot{u}_n = \frac{1}{\Delta t_n}(u_{n+1/2} - \dot{u}_{n-1/2}), \tag{27}$$

displacement at t_{n+1}: as:

$$(\frac{1}{\Delta t^2}M_n + \frac{1}{2\Delta t}C_n)u_{n+1} = p_n - (K_n - \frac{2}{\Delta t^2}M_n)u_n - (\frac{1}{\Delta t^2}M_n - \frac{1}{2\Delta t}C_n)u_{n-1}. \tag{28}$$

If the matrices M and C are diagonal, matrix inversion is not required. The solution is simple and quick. The disadvantage of this method is its conditional stability.

4. Simulation results

Using a theoretical analysis of the dynamic interactions with respect to detonation of the basic material, numerical simulations of 400 g TNT charge explosion were carried out. The load was placed at a depth of 10 meters, 25 meters from the hull of boats with a displacement of D = 800 kg.

The results were compared with another experiment, presented in Fig. 7-8. The obtained results of the acceleration and its simulation from the pressure of the shock wave are shown on Fig. 9-10.

The results of testing and proving ground simulation provide the basis for the implementation of a virtual model of ship hull subjected to impulse loads.
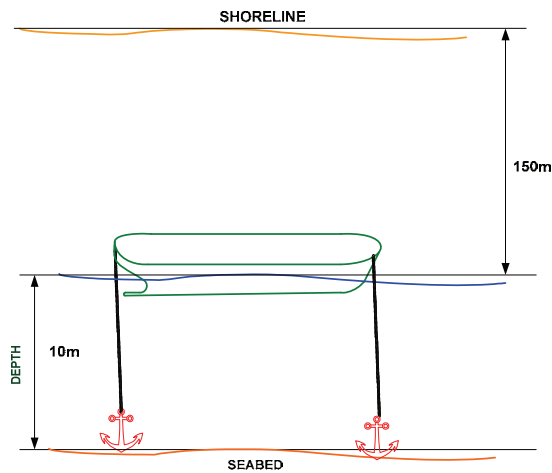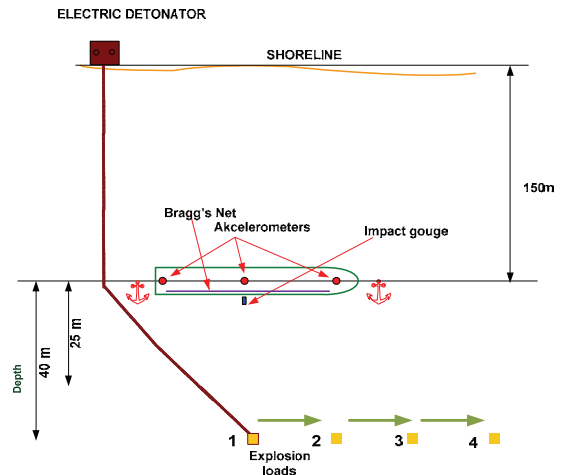
Fig. 7. Schematic anchor launch

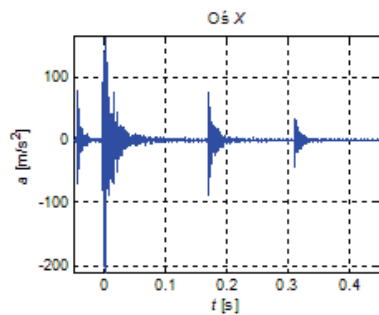Fig. 8. Layout of the apparatus and the conditions for an explosion

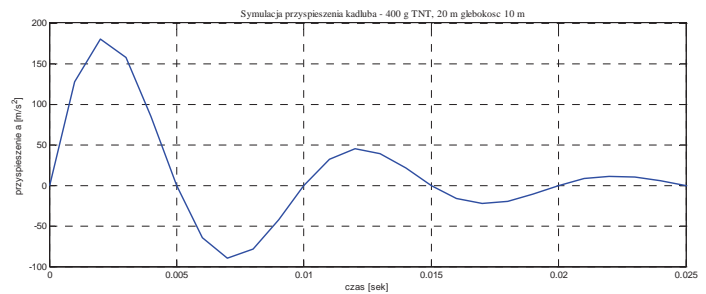Fig. 8. The course of the accelerations recorded in the ship's hull

Fig. 9. The course of simulation of the acceleration

5. Conclusion

Modelling the dynamic interaction of the detonation of underwater hull of the ship is a difficult and long process. The results of the first simulation, which emulates ideal conditions without the influence of the seabed and sea surface in the shape of the pulse will cause a rise to many errors. It should be emphasized that the purpose of this research is not an exact reflection of interactions, but attempting to answer one particular question: What order of pressure occurs in the construction of the hull subjected to shock loads?. The aim of this study is to identify risks from excess of pressure tolerated in the internal nodes of the hull, which are the bearings of marine propulsion, technical equipment and armaments.

References

[1] Cole, R. H., *Underwater explosions*, Princeton University Press, 1948.
[2] Young, S., Shin, *Ship shock modeling and simulation for far-field underwater explosion*, Computers and Structures, 82, pp. 2211–2219, 2004.
[3] DeRuntz, Jr, J. A., *The underwater shock analysis code and its application,* Proc 60th Shock Vib Symp, 1: 89–107, 1989.
[4] Costanzo, F. A, Gordon, J. D., *An analysis of bulk cavitation in deep water*, DTNSRDC, UERD Report, May 1980
[5] Hallquist, J. O., *LS-DYNA Theoretical Manual*, Livermore Software Technology Corporation, Livermore, CA 1998.
[6] Malone, P. E, Shin, Y. S., *Sensitivity analysis of coupled fluid volume to ship shock simulation*, Proc 71st Shock Vib Symp, 2000.